Investigation of On-chip Temperature Measurement in Power Cycling Using Fibre Bragg Grating Sensors

Mark Sherriff PEMC Research Institute University of Nottingham Nottingham, U.K. mark.sherriff@nottingham.ac.uk

Paul Evans PEMC Research Institute University of Nottingham Nottingham, U.K. paul.evans@nottingham.ac.uk

Ricardo Correia Optics and Photonics Group University of Nottingham Nottingham, U.K.

ricardo.goncalvescorreia@nottingham.ac.uk

Chenyang He Optics and Photonics group University of Nottingham Nottingham, U.K. chenyang.he2@nottingham.ac.uk

Ke Li PEMC Research Institute University of Nottingham Nottingham, U.K. ke.li2@nottingham.ac.uk

Abstract—Condition monitoring techniques underpin the successful drive towards the net zero economy, providing more accurate predictive maintenance for electrical infrastructure and hence increasing system service life. Fibre Bragg grating (FBG) sensors provide an electrically isolated temperature measurement, which can be utilized for fast and accurate semiconductor junction temperature estimation. Compared with traditional temperature-sensitive electrical parameters, FBG temperature measurement is immune to electromagnetic interference and is not affected by device ageing. In this paper, the procedure of on-chip FBG temperature measurement is presented in the context of power cycling for silicon diode test vehicles. Accuracy of the sensor transient response is discussed, alongside mitigating factors and potential avenues for future improvements.

Keywords—condition monitoring, fibre Bragg grating, reliability, temperature-sensitive electrical parameter, power semiconductor lifetime.

I. INTRODUCTION

Fast and accurate estimation of device junction temperature (T_i) within power electronics modules (PEMs) is critical to the mitigation of unscheduled maintenance expenses. Swings in T_i caused by periodic heating and cooling from operation creates thermomechanical stresses within the device arising from mismatches in the coefficients of thermal expansion (CTEs) of its constituent materials [1]. The structure of a typical power module is shown in Fig. 1. Thermomechanical stress leads to degradation, reducing the service life of devices, often leading to catastrophic and costly failure of power electronics systems. The push towards a net zero economy by 2050 will benefit greatly from developments in condition monitoring (CM) techniques, allowing accurate estimation of device remaining useful life (RUL) to drive predictive maintenance schemes.

Common to the packaging of some high-voltage power module platforms is the inclusion of negative temperature coefficient (NTC) thermistors, which allow for temperature monitoring at the package substrate. The drawback of this approach is that the thermistors are located far from the devices and consequently lead to poor inference of T_i . Another widely adopted approach for T_i measurement is the use of semiconductor temperature-sensitive electrical

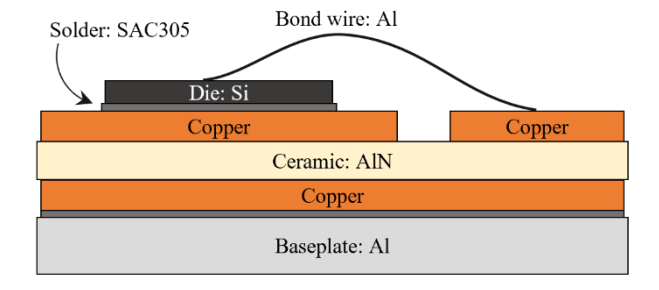


Fig. 1 Typical structure of power electronics module.

parameters (TSEPs), offering far greater accuracy than the use of embedded NTC thermistors. Measurable at the device terminals, TSEPs are specific to device technology, package layout, and can vary with device ageing [2]. Notable TSEPs include device on-state voltage ($V_{CE(on)}$), gate threshold voltage (V_{th}) , turn-on and turn-off switching times (t_{on}, t_{off}) , and switching delay times $(t_{d(on)}, t_{d(off)})$ in silicon insulated gate bipolar transistors (IGBTs) [3]. Wide bandgap (WBG) devices offer higher operating temperatures, blocking voltages and switching speeds, and are being leveraged to create ever more efficient power electronics systems. However, they require device-specific TSEPs for accurate T_i estimation [4]. Another factor worth noting is the degradation of TSEP due to semiconductor device aging and degradation. Consequently, a significant amount of work is involved in the calibration of dedicated TSEPs, which are not universally applicable to power electronics devices and challenge their applications for real-time on-line monitoring.

The use of fibre Bragg grating (FBG) sensors to monitor the junction temperature of semiconductor devices is an emerging technology for power electronics condition monitoring. An optical fibre-based temperature sensor can be integrated into the device or module packaging at the manufacturing stage or retroactively, providing an electrically isolated and precise real-time temperature measurement close to the device junction. Notably, this approach is independent of device technology and requires only access to the semiconductor dies. As WBG devices are operated with fast slew rates, it is advantageous that the FBG-based approach is immune to the ensuant electromagnetic interference (EMI). Recently, FBG temperature measurement approaches have been applied in the baseplate underneath power semiconductor devices [5], demonstrating the capability of a single fibre for distributed temperature measurement. This was later applied to IGBT press-pack modules, where the

Funded by the European Union under GA no. 101172794, International Science Partnerships Fund and the UK Research and Innovation under the reference EP/Y002261/1. Views and opinions expressed are however those of the authors only and do not necessarily reflect those of the European Union or CINEA. Neither the European Union nor the granting authority can be held responsible for them.

sensors were integrated into molybdenum platelets for in situ chip temperature measurement [6]. Other researchers investigated the applicability of the FBG technology for onchip temperature measurement in insulated gate bipolar transistor (IGBT) power modules [7], [8], [9]. The positioning and interfacing of the sensing head were studied, finding that a high quality, yet yielding, thermal interface positioned at the hot spot of the device improved measurement accuracy and transient response.

In comparison to the above work, the main contribution of this paper is to offer a detailed analysis of calibration, implementation and measurement error of using FBG sensors for power cycling of power semiconductor devices, which offers additional data for their industrial application. The paper is constructed from the following sections. First, the calibration procedure for unstrained FBG sensors is discussed, comparing two common models. After that, experimental results for on-chip temperature measurement during a power cycling application are then shown with varying cycle times, comparing the measurement error between FBG-based sensor and mid-wave infrared (MWIR) thermal imaging. Finally, the transient response error is highlighted, alongside a potential mitigating approach where the fibre jacket is removed to reduce thermal resistance in the measurement chain.

II. FBG SENSOR CALIBRATION

A. Fibre-Bragg Grating Temperature Sensors

A functional FBG sensor is created by a periodic inscription of the core of an optical fibre, serving to adjust its refractive index at those points. The fibre reflects light of the central Bragg wavelength, λ_B , related to the period of the grating, Λ , by (1), and transmits other light [9], [10].

$$\lambda_B = 2 \cdot \Lambda \cdot n_{eff} \tag{1}$$

where n_{eff} is the effective refractive index of the fibre.

Variation of the temperature, ΔT , or strain, $\Delta \varepsilon$, acting upon the fibre causes a commensurate variation in the reflected wavelength, $\Delta \lambda_B$, given by (2).

$$\Delta \lambda_B / \lambda_B = \Delta T(\alpha + \xi) + \Delta \varepsilon (1 - p_{eff})$$
 (2)

where α is the thermal expansion coefficient of the fibre, ξ is the thermo-optic coefficient of the fibre, and p_{eff} is the photo-elastic constant for the fibre.

In a constant strain or strain-free configuration for the sensing head, the reflected wavelength is sensitive only to variation in temperature, as represented by (3) [9].

$$\Delta \lambda_B = \lambda_B \cdot \Delta T \cdot (\alpha + \xi) \tag{3}$$

Other authors have reported a calibrated sensitivity for similar sensors of $10{\text -}14~\text{pm}\cdot^\circ\text{C}^{-1}$. Key geometric features for a typical FBG are shown in Fig. 2. The sensors selected for this work were fabricated from Corning SMF-28e+ optical fibre, inscribed with a 3 mm sensing head. The diameters of the fibre core, acrylate cladding, and acrylate jacket were $8.2~\mu\text{m}$, $125~\mu\text{m}$ and $250~\mu\text{m}$, respectively. The cladding allows operation of the optical fibre due to the difference in the refractive index from the fibre core, and the jacket provides mechanical strength.

B. Calibration of FBG Sensors

In a constant strain configuration, the reflected wavelength is changed only by variation in the ambient temperature.

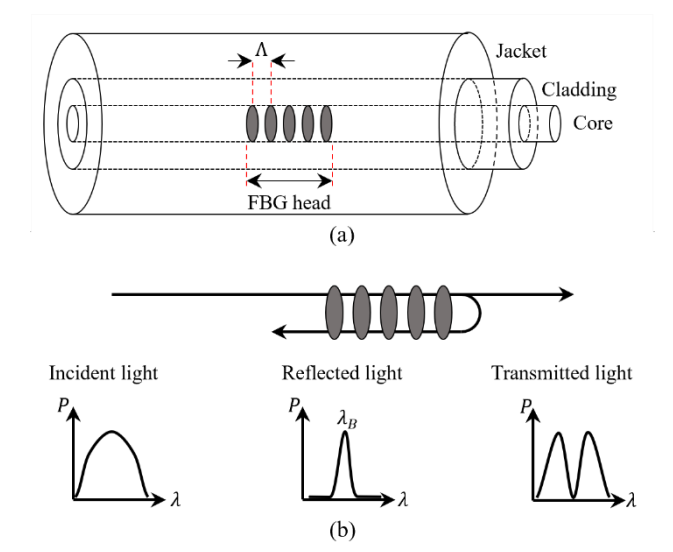


Fig. 2 FBG characteristics: (a) structure, (b) light propagation.

Consequently, calibration of the sensors to determine the wavelength-to-temperature relationship is possible through heating the fibre to increasing temperatures, pausing until steady-state is achieved at each stage. The $\lambda-T$ mapping is then performed using an appropriate model.

For this work, FBGs were placed in a programmable temperature chamber (ESPEC BTZ-175E) alongside thermocouples atop a metal heatsink to provide a thermal mass, and subjected to periodically increasing temperatures in the range 40–160 °C. The fibre was fastened at one end only to ensure no strain was induced at the point of the sensing head. Fig. 3 shows fitting results for linear and quadratic models given by (4) and (5), respectively, following the approach of other authors [5], [8]. Fitting results are also presented for clarity in Table I.

$$T_L = p_1 + p_2 \cdot (\lambda - \lambda_B) \tag{4}$$

$$T_0 = p_1 + p_2 \cdot (\lambda - \lambda_B) - p_3 \cdot (\lambda - \lambda_B)^2 \tag{5}$$

where T_L and T_Q are the temperature estimates for the linear and quadratic models, respectively, p_1 , p_2 and p_3 are fitting parameters, and λ is the measured wavelength.

FBG CALIBRATION FITTING RESULTS

Model	p_1	p_2	p_3	Adj-R ²
Linear, (4)	24.7253	88.8675	_	0.9993
Quadratic, (5)	22.2313	98.2138	5.6986	0.9999

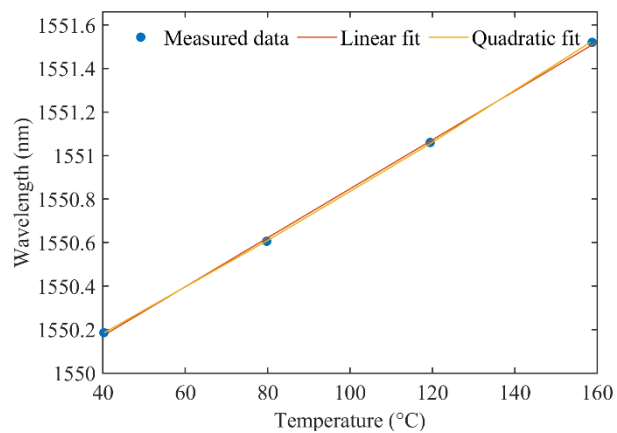


Fig. 3 Calibration results for FBG sensor with linear and quadratic models.

Although the model of (4) provides good linearity, the model of (5) was selected for use in this work due to the higher adjusted-R².

III. TEMPERATURE MEASUREMENT UNDER POWER CYCLING

A. Experiment Procedure

Silicon diodes were selected as test vehicles for this work. Diode dies were soldered to active metal brazed (AMB) aluminium nitride (AlN) substrate tiles before aluminium wire bonds (370 μm diameter) were attached to complete the sample. The diode test vehicles were then connected to bespoke power cycling equipment. A constant current is applied to samples while the die temperature is monitored with infrared pyrometers. The equipment allows the sample to be heated by the test current until an upper temperature limit is reached, whereupon the heating current is diverted, allowing samples to be cooled via the cold plate The chiller attached to the cold plate is fixed at 20 °C for all testing.

The die surface temperature was recorded during initial cycling trials with a MWIR thermal camera (CEDIP Titanium) to determine the optimal position of FBG sensors, following the approach of other authors for similar work [7]. To ensure correct operation of the power cycling equipment and so that the MWIR could accurately record sample temperatures, matte black paint was applied to the die surface. FBG sensors were placed in the centre of the die, commensurate with the locus of heat generation as recorded by the MWIR imaging. Fig. 4 shows thermal imaging of the die surface under 60 A heating current, clearly highlighting the centre of the die as the hotspot and a clear positioning target for the FBG sensing head.

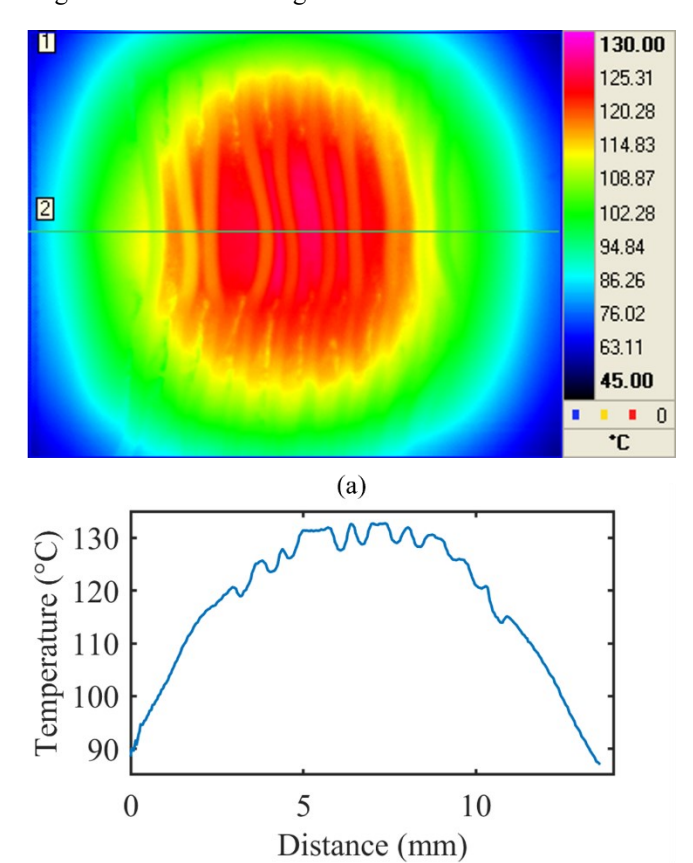


Fig. 4 MWIR thermal imaging during heating transient: (a) die surface image, (b) temperature profile of line 2 across die surface.

(b)

Layers of Kapton tape were used to raise the FBG sensors from the substrate level to ensure the sensing head was close to the die surface. The fibre was then fastened in place with more tape, leaving one end free. A photograph of a prepared sample in situ of the power cycling equipment is shown in Fig. 5. An advantage of such fixture is the strain free arrangement of the sensor head, which avoids measurement error due to strain stress. However, a tiny airgap of a few tens of micrometers could be presented between the die chip and sensor head, which influences measurement accuracy. This will be further investigated in the sections below.

Fig. 6 shows a comparison between the temperatures recorded by the MWIR thermal camera and from the interpreted FBG measurement, for a heating current of 40 A with heating limits 40–90 °C. Although at the start and end of the heating cycle the error may be within acceptable tolerances, depending on the application, the error during the heating period is significantly greater, and is further investigated below.

B. Transient Response With Varied Cycle Times

The influence of cycle time on the transient response of the FBG sensors was investigated by fixing the power cycling minimum and maximum temperatures to 40 °C and 90 °C, respectively, and varying the heating current. With lower heating current, the system takes longer to reach the target temperature, allowing for lengthened heating of the fibre jacket and cladding. Conversely, more rapid power cycling limited the heating of the fibre outside the core and was expected to result in greater transient measurement error.

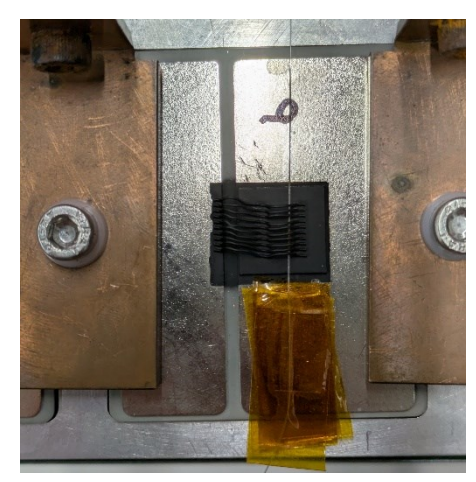


Fig. 5 Photograph of diode test vehicle with FBG sensor attached, in situ of power cycling equipment.

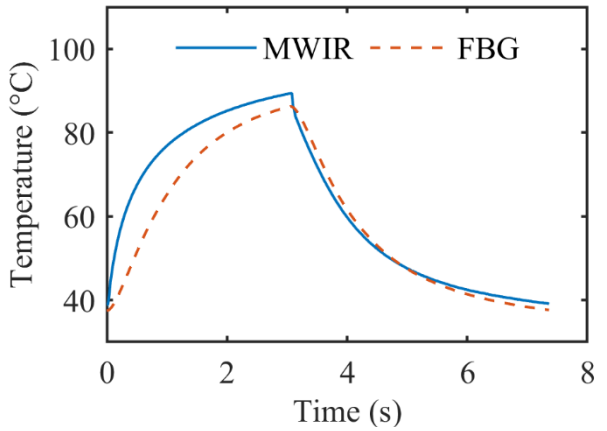


Fig. 6 Comparison of measured chip temperature (MWIR) and interpreted FBG temperature measurement (FBG) under power cycling at 40 A.

A series of cycling trials with heating currents increasing from 35 A to 60 A were performed to evaluate the transient thermal response for different heating and cycle times. The same minimum and maximum temperatures were kept from before for ease of comparison. Fig. 7 shows the temperature measurement errors for different heating currents. As heating current is increased and heating times reduced, the maximum temperature measurement error is significantly increased. It is also observed that as the heating current is increased, the errors at the maximum temperature (90 °C) and the maximum error during heating converge. This is demonstrated further in Fig. 8, showing how decreasing heating time serves to increase the temperature measurement error at these points. Simulations of a similar scenario but with fixed duty cycle were shown in [7], which demonstrated that increasing the switching frequency of a device under power cycling reduced the average temperature within the sensing head of an FBG sensor above the die.

IV. FBG TRANSIENT RESPONSE IMPROVEMENT THROUGH REMOVAL OF JACKET

As discussed in [6], the material surrounding the FBG has a significant influence on the transient response. This is also investigated in [7], where an air-gap between the FBG and die resulted in larger error compared to a solid thermal interface. This was developed further in [8], with an investigation into adhesives for FBG-die bonding. Subject to appropriate calibration methods, these works found that the thermal interface provided no additional strain-induced error. However, the reliability of the interface considering ageing

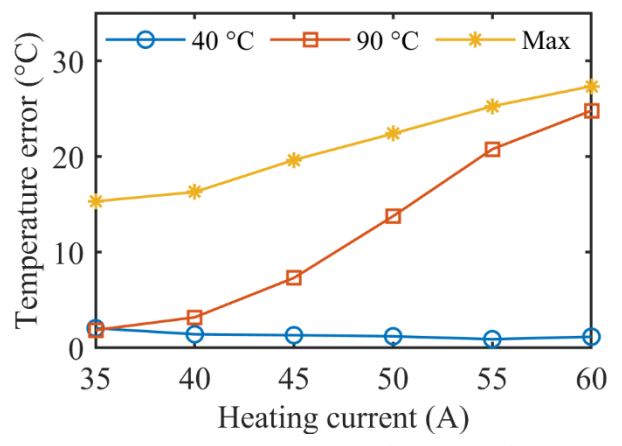


Fig. 7 FBG temperature measurement error for increasing heating current. (o) error at 40 °C, (\square) error at 90 °C, (*) maximum error during heating.

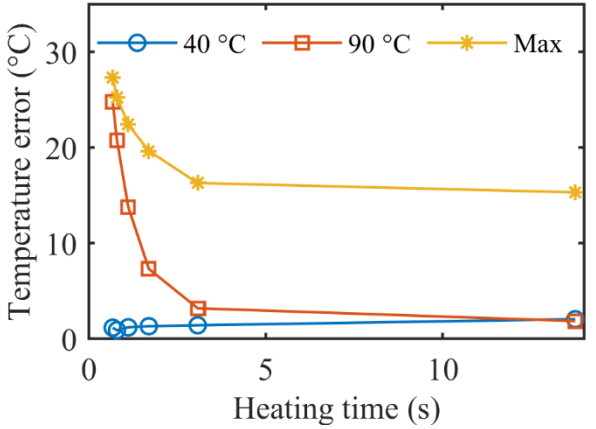


Fig. 8 FBG temperature measurement error against heating times. (o) error at 40 °C, (\square) error at 90 °C, (*) maximum error during heating.

during device operation is not yet understood. Consequently, error mitigation methods that do not rely on the addition of a thermal interface material may be desirable from a point of view of longevity and could increase flexibility in the design of condition monitoring approaches.

A. Simulation of FBG Response With and Without Jacket

Placement of the sensor close to the die is not always easily achieved considering a retrofit of the sensor into already built modules, which could lead to increased temperature measurement error. Even if the sensor can be placed on the die, previous work has shown the importance of accurate positioning atop the die and of the FBG head size, adding additional complexity to the attachment process [11]. Initial 2D transient thermal simulations were performed in ANSYS Fluent to evaluate the influence of physical displacement from the die surface with no FBG present. An annotated diagram of the simulation geometry is shown in Fig. 9, which indicates also the positioning of the FBG for subsequent simulations. All simulations make use of a symmetry boundary condition to aid in computation time and convergence, so only half of the geometry is modelled. The side and top of the air domain are set to a convection boundary condition with a heat transfer coefficient of 10 W·m⁻²·K⁻¹. The ambient, free stream and initial temperatures are set to 20 °C. The temperature of the die is set to follow the transient temperature profile recorded by thermal imaging during power cycling at 40 A.

Fig. 10 shows temperatures recorded at the mid-point of the die surface and at 50 μ m, 100 μ m and 200 μ m from the die surface. Air further away from the die is shown to be cooler overall during power cycling. In all cases the maximum temperature difference between the point in air and the die is at the peak of the heating period. In a similar result to that of other works [7], this indicates that a sensor placed away from the die surface is expected to experience a cooler average temperature during cycling, even without factoring in the thermal impedance of the jacket and cladding.

The primary purpose of the jacket around the FBG is to provide mechanical strength, since the fibre core alone is fragile and easy to damage. To evaluate the potential for transient thermal error reduction by stripping the fibre jacket away, additional simulations were performed with an FBG positioned 50 μ m from the die surface. The fibre is modelled according to the manufacturer geometry, using polymethyl methacrylate (PMMA) for the cladding and jacket, and silica

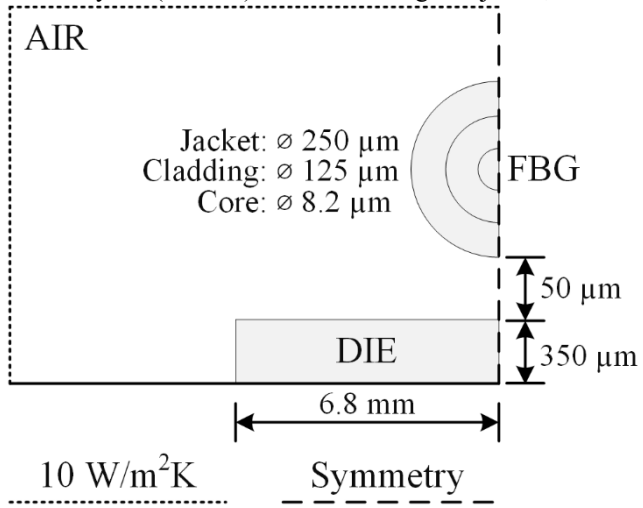


Fig. 9 Diagram of ANSYS Fluent 2D simulation geometry. Dimensions exaggerated for clarity. Model air domain is 50 mm wide and 75 mm high.

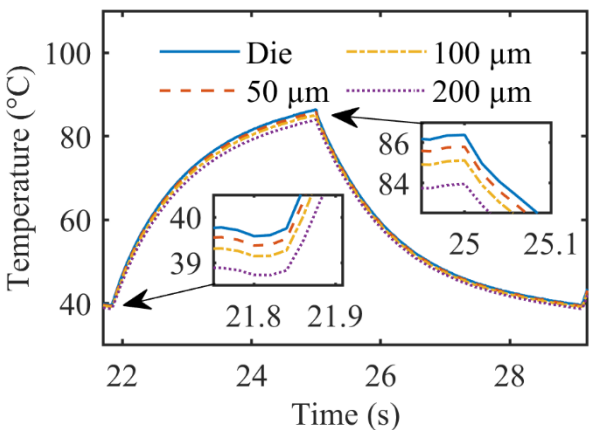


Fig. 10 Simulation thermal profiles in air above die under power cycling. Simulation performed with no FBG present.

glass for the fibre core. Following the approach of other work [7], the mean temperature of the fibre core is used to evaluate the FBG thermal response with and without the fibre jacket. The resultant simulation thermal profiles are shown in Fig. 11, demonstrating that the bare FBG (i.e. with the jacket removed) exhibits a lower temperature measurement error during power cycling than the FBG complete with jacket. This indicates an opportunity for simple error mitigation for FBG-based direct die temperature measurement, even in scenarios where an air gap between die and sensor is difficult to avoid.

B. Jacketless FBG Response During Power Cycling

Practical removal of the fibre jacket easily done with wellcalibrated stripping tools and was investigated in this work by placing the sensing head atop the die in the same arrangement as in the above subsection, aiming to ensure contact between the fibre cladding and the die surface. The same $\lambda - T$ calibration shown in § II is used for the no-jacket case due to the free arrangement of the fibre. Fig. 12 shows results under power cycling at 40 A in the range 40–90 °C. Table II shows the temperature measurement error at key times during the heating period for power cycling at 40 A with and without fibre jacket in the free arrangement (i.e. fixed at one end only), including simulation (sim.) and experimental (exp.) results. For the experimental results, stripping the jacket is revealed to reduce the maximum error during power cycling to 9.66 °C from 16.30 °C at the same heating current without the jacket stripped, an effective worst-case error reduction of 40.74%.

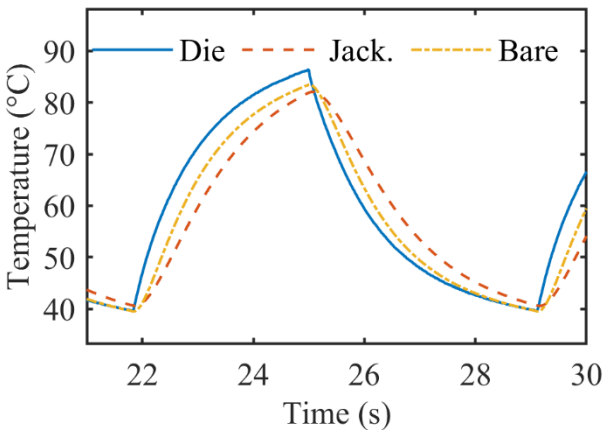


Fig. 11 Simulation thermal profiles of the die (blue, solid), FBG core with jacket (orange, dashed) and FBG core without jacket (yellow, dash-dot) under power cycling.

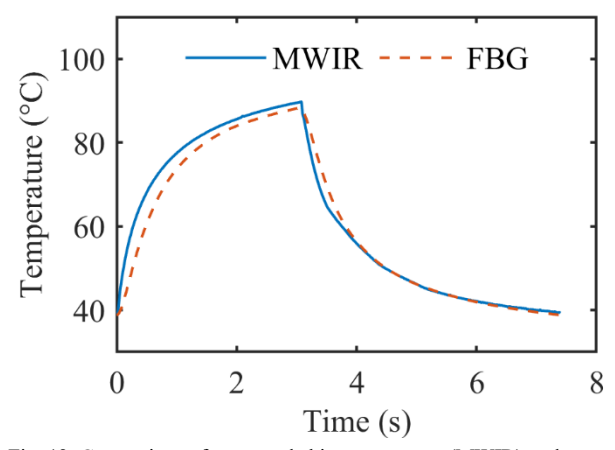


Fig. 12 Comparison of measured chip temperature (MWIR) and interpreted FBG temperature measurement (FBG) under power cycling at 40 A, using jacketless sensor.

 $\label{eq:Table II} FBG\ Transient\ Error\ With\ and\ Without\ Jacket\ at\ 40\ A$

Jacket	Error at 40 °C (°C)	Error at 90 °C (°C)	Max. temp. error (°C)
Yes (sim.)	1.03	4.45	12.65
Yes (exp.)	1.44	3.21	16.30
No (sim.)	0.08	2.92	8.24
No (exp.)	0.37	1.45	9.66

Similar trends are observed in the simulation results, with a reduction from 12.65 °C to 8.24 °C at the point of maximum error (-34.86%). Good agreement is reached between experiment and simulation, indicating that the effective air gap of the FBG and die surface in the experiment was close to the 50 μm assumed for the simulation. Although efforts were made to ensure a contact between the FBG and die in the experiment, it was not possible to practically measure the air gap across the length of the FBG.

V. CONCLUSION

This work presents an easily implemented method for mitigating the error in on-chip temperature measurement using FBG sensors by way of removing the fibre jacket. A silicon diode soldered to an AlN AMB substrate tile is used as a representative sample for measurement of chip temperature under power cycling operation, indicative of field operation of power semiconductor devices. The procedure for calibration of FBG sensors fastened at one side of the die to be measured (i.e. a free arrangement) is presented, and comparison is made between two models for $\lambda-T$ mapping. In this work, the quadratic model is chosen over the linear model due to the increased fit accuracy.

Practical experimentation is performed with calibrated FBGs on the diode samples under power cycling in the temperature range 40–90 °C. MWIR thermal imaging was used to locate the hotspot of the die during thermal transient to select the optimal position of the sensor for the experiments. An analysis of transient thermal error showed that a short heating times caused by increased heating current resulted in a significantly increased error in the interpreted FBG temperature measurement compared to the MWIR-recorded die surface temperature. Consequently, exploration of methods to reduce the transient thermal error were carried out through simulation (ANSYS Fluent) and practical

experimentation. The air gap between the FBG and die is highlighted as a target for improvement, and in other works this is mitigated via a thermal interface adhesive.

Aiming to provide an alternative method, this work pursued an approach whereby the effective thermal impedance of the FBG itself is reduced by removing the fibre jacket. This is easily achieved in practice, and results with good agreement between simulation and experimentation indicate that the approach is able to reduce the temperature measurement error during power cycling. This provides flexibility for future condition monitoring approaches with the use of FBGs for on-chip temperature measurement, affording system designers the opportunity to select sensors that are free from electromagnetic interference.

ACKNOWLEDGEMENT

The authors would like to think the FLAGCHIP consortium members for their guidance and technical input.

REFERENCES

- [1] H. Ren *et al.*, "Research on the Electro-Thermal–Mechanical Properties of IGBT Modules Under Different Bond Wire Failure Modes," *IEEE Transactions on Electron Devices*, vol. 71, no. 7, pp. 4259-4266, 2024, doi: 10.1109/ted.2024.3404417.
- [2] J. Li, Y. Sha, M. Zhou, and L. Wang, "Analysis of the Influence of Bond Wire Aging on Junction Temperature Estimation in IGBT Modules," in *IEEE 7th International Electrical and Energy Conference (CIEEC)*, 2024 2024: IEEE, doi: 10.1109/cieec60922.2024.10583390. [Online]. Available: https://dx.doi.org/10.1109/cieec60922.2024.10583390
- [3] M. H. M. Sathik, J. Pou, S. Prasanth, V. Muthu, R. Simanjorang, and A. K. Gupta, "Comparison of IGBT junction temperature measurement and estimation methods-a review," in 2017 Asian Conference on Energy, Power and Transportation Electrification (ACEPT), 24-26 Oct. 2017 2017, pp. 1-8, doi: 10.1109/ACEPT.2017.8168600.
- [4] H. Wen *et al.*, "Junction Temperature Extraction for Silicon Carbide Power Devices: A Comprehensive

- Review," *IEEE Transactions on Power Electronics*, vol. 40, no. 2, pp. 3090-3111, 2025, doi: 10.1109/tpel.2024.3486149.
- [5] A. Mohammed *et al.*, "Distributed Thermal Monitoring of Wind Turbine Power Electronic Modules Using FBG Sensing Technology," *IEEE Sensors Journal*, vol. 20, no. 17, pp. 9886-9894, 2020, doi: 10.1109/jsen.2020.2992668.
- [6] H. Ren *et al.*, "Quasi-Distributed Temperature Detection of Press-Pack IGBT Power Module Using FBG Sensing," *IEEE Journal of Emerging and Selected Topics in Power Electronics*, vol. 10, no. 5, pp. 4981-4992, 2022, doi: 10.1109/JESTPE.2021.3109395.
- [7] S. Chen, D. Vilchis-Rodriguez, S. Djurović, M. Barnes, P. Mckeever, and C. Jia, "Direct on Chip Thermal Measurement in IGBT Modules Using FBG Technology—Sensing Head Interfacing," *IEEE Sensors Journal*, vol. 22, no. 2, pp. 1309-1320, 2022, doi: 10.1109/JSEN.2021.3131322.
- [8] S. Chen, D. Vilchis-Rodriguez, M. Barnes, and S. Djurović, "Direct On-Chip IGBT Thermal Sensing Using Adhesive Bonded FBG Sensors," *IEEE Sensors Journal*, vol. 23, no. 19, pp. 22507-22516, 2023, doi: 10.1109/JSEN.2023.3301070.
- [9] S. Chen, D. Vilchis-Rodriguez, M. Barnes, and S. Djurović, "Direct sensing of IGBT junction temperature using silicone GEL bonded FBG sensors," in 12th International Conference on Power Electronics, Machines and Drives (PEMD 2023), 23-24 Oct. 2023 2023, vol. 2023, pp. 329-334, doi: 10.1049/icp.2023.2019.
- [10] J. A. Bradbury *et al.*, "Fibre Bragg Grating Based Interface Pressure Sensor for Compression Therapy," *Sensors*, vol. 22, no. 5, p. 1798, 2022, doi: 10.3390/s22051798.
- [11] S. Chen, D. Vilchis-Rodriguez, S. Djurović, M. Barnes, P. McKeever, and C. Jia, "FBG Head Size Influence on Localized On-Chip Thermal Measurement in IGBT Power Modules," *IEEE Sensors Journal*, vol. 22, no. 22, pp. 21684-21693, 2022, doi: 10.1109/JSEN.2022.3210708.